MONTE CARLO RADIATION TRANSFER MODELS FOR MARS. B. A. Whitney[1], M. J. Wolff[2], and R. T. Clancy[3], Space Science Institute, 1540 30th St., Suite 23 Boulder, CO 80303-1012, [1]bwhitney@colorado.edu, [2]wolff@colorado.edu, [3]clancyr@colorado.edu .

Introduction: We have developed a 3-D Monte Carlo radiation transfer code to aid in the analysis of several currently available datasets for Mars. Our code uses algorithms developed previously for other applications [1],[2],[3],[4],[5]. The code accurately computes scattering and thermal emission in the Martian atmosphere and surface. Any number of opacity sources may be specified for the atmosphere. The Monte Carlo algorithms calculate complicated dust scattering functions with the same ease as isotropic. The surface scattering properties currently use the Minneart law for phase function. In contrast to a plane-parallel radiation transfer model, this code calculates the radiation transfer of the planet as a whole with incident solar radiation. The surface and atmospheric properties can be specified in a 3-D grid, allowing for surface features and clouds to be repesented in model images. The solar angle and the viewing angle are arbitrarily specified. The code allows viewing of the planet from several vantage points, to allow for more direct comparison to datasets produced by the Hubble Space Telescope, the Mars Global Surveyor, and the Mars Pathfinder.

Examples of the Mars Code: This section presents examples to show the capabilities of the code. Figure 1 shows a model image of Mars viewed from the earth with the resolution typical of the Hubble Space Telescope (HST). This model uses a 1042 nm surface reflectance map [6]. We will make direct comparisons to HST images by convolving the model images with the HST point spread function. An example of an initial study we are undertaking is to model atmospheric Ozone abundances of mars by comparing models to HST images taken in the Hartley band. Our study will focus on the limb. Figure 2 shows model predictions. This model includes ozone, cloud, rayleigh and dust opacities. The multi-year coverage of the HST data (1995-7) provides information about the latitudinal, seasonal, and interannual variations of Martian ozone column densities. We will focus our efforts on the period from late spring through the end of summer (in the northern hemisphere), with special attention given to low-to-mid latitude regions where coverage is very incomplete.

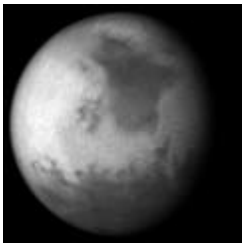

Figure 1. Model image of Mars. The atmosphere has a dust optical depth of 0.4. Subsolar and Subearth points are arbitrarily chosen to be (lat=25,lon=80) and (lat=25,lon=40) respectively.

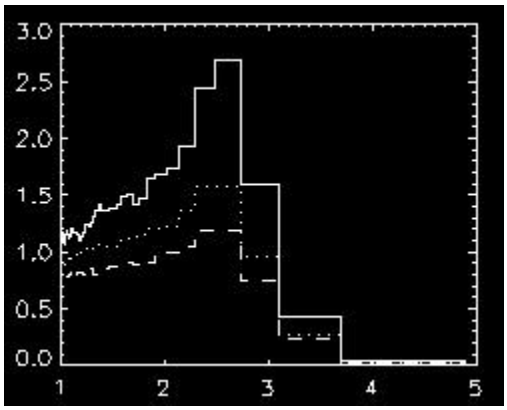

Figure 2. A scan across the disk of three models is plotted as Flux vs. Air Mass (the pixel size varies for equal units of air mass). The models vary the amount of Ozone from 0 (solid line), 2 (dotted), and 4 (dashed) μ-atm. The flux is normalized to the center of the disk of the 0 μ-atm model. It is the attenuation of the limb brightening due to Ozone that we wish to measure by comparing to HST images. This change in brightness at the limb is noticeable, well within the 5% photometric accuracy of the WFPC2 camera at this wave-

Using various algorithms for weighting and forcing photon direction [7], we can calculate the amount of radiation incident on a particular place within the atmosphere, for example, from the Pathfinder or the Mars Global Surveyor. Figure 3 shows a view from the Pathfinder. We plan to study the distribution of scattered light on the sky and the dust scattering prop-

Figure 3. An example 3-color (red-blue-green) image viewed from the surface. The sun is to the right in the image. The azimuthal view covers 360 degrees and the zenith angle ranges from –60 to +60. The atmospheric and surface properties are shown in Table 1.

erties. We will investigate the unexpectly long twilight phenomenon measured by Pathfinder[8]. We will vary the scattering properties of the dust, within reason, to determine if we can reproduce the brightness via dust scattering at high levels in the atmosphere.

Wavelength	410 nm	502 nm	673 nm
Dust albedo	0.64	0.75	0.93
Dust $\langle\cos\theta\rangle$	0.78	0.73	0.68
Dust optical depth	0.376	0.4	0.42
Surface albedo	0.04	0.06	0.25

Table 1. Scattering properties

An example Mars Global Surveyer view is shown in Figure 4. Since this image was made, we have improved the signal-to-noise significantly, by placing more incident photons in the region of interest and weighting them accordingly.

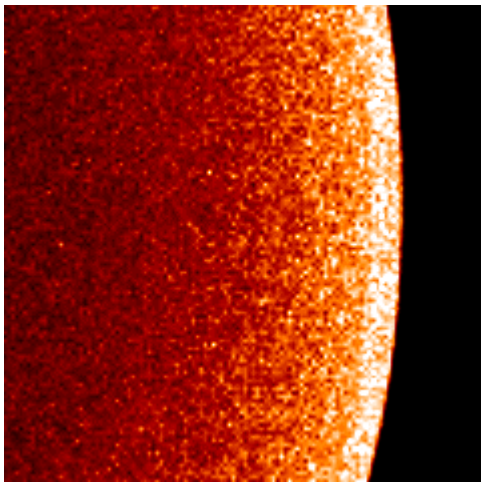

Figure 4. A view of the martian limb from an altitude of 400 km. This image was produced using the scattering properties Table 1 for a wavelength of 673 nm.

Figure 5 shows thermal emission images for 3 different incident solar angles. The temperature of the planet is assumed to follow a cosine law (of the solar angle) for this model, but can be arbitrarily defined in the code. The thermal emission capabilities are still in development. Our goal is calculate thermal emission from the atmosphere and surface from a viewpoint of the Mars Global Surveyor for limb studies. We hope to have this completed by summer of 1999.

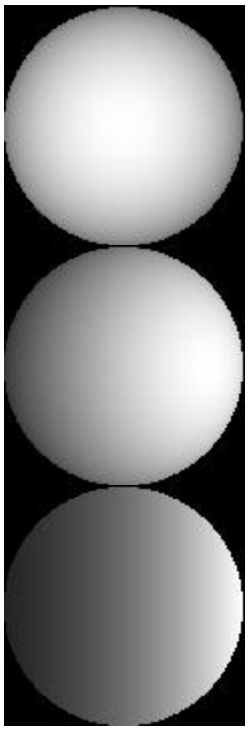

Figure 5. Thermal emission images of the surface for 3 different solar angles. The top image has the viewing angle the same as the sun. The middle and bottom images have the sun 45 and 90 degrees from the viewing angle, respectively.

References: [1] Whitney B. A. (1991) *ApJS, 75*, 1293-1322. [2] Whitney B. A. (1991) *ApJ.,369*, 451-462. [3] Whitney B. A. and Hartmann L. (1992) *ApJ*, 529-539. [4] Whitney B. A. and Hartmann L. (1993) *ApJ, 402*, 605-622. [5] Code A. D. and Whitney B. A. (1995) *ApJ, 441*, 400-407. [6] Bell J. F. et al. (1997) *JGR, 102*, 9109–9124.. [7] Smith P. H. et al. (1997) *Science 278*, 1758-1765.